



# Assessment of water inrush risk based comprehensive cloud model: a case study in a lead zinc mine, China

Qiang Li<sup>1,2</sup> · Wanghua Sui<sup>1</sup> · Bangtao Sun<sup>3</sup>

Accepted: 2 November 2022 / Published online: 24 November 2022

© The Author(s), under exclusive licence to Springer-Verlag GmbH Germany, part of Springer Nature 2022

## Abstract

This paper presents a water inrush comprehensive evaluation model based on cloud model. The qualitative and quantitative transformation of water inrush evaluation indices are realized by cloud generator, applied in the water inrush risk evaluation of lead zinc ore body mining in karst aquifer. 9 factors were selected to construct the water inrush evaluation index system. The risks of water inrush were classified to five levels: risk level I, risk level II, risk level III, risk level IV and risk level V, respectively. The improved analytic hierarchy process (IAHP) and the criteria importance through intercriteria correlation (CRITIC) were adopted to determine the subjective and objective weights of the evaluation indicators, respectively. The concept of Kullback information was applied to determine the combination weight of evaluation indices. Then, the comprehensive certainty of the water inrush risk level was determined, combining the index weight and the corresponding cloud eigenvalue. In addition, combined with the water inrush risk level of the samples, the water inrush risk zoning of the study area was realized with geographic information system (GIS). This model was applied to the Maoping lead zinc mine in southwestern China to evaluate the risk of water inrush from the mining of the ore body. The results show that the combined weight method (CWM) based on the concept of Kullback information is characteristic by both subjective and objective, without weight bias; the cloud model can better convert the qualitative and quantitative between evaluation indices; the prediction accuracy of the water inrush evaluation model constructed based on the CWM is higher than that of IAHP, CRITIC and water inrush coefficient (WIC), with a better fitting effect. This work provides an innovative idea for water inrush evaluation of ore body mining in karst aquifers.

**Keywords** Water inrush · Mine · Cloud model · Risk assessment · Karst

## Introduction

The lead and zinc, as a category of non-ferrous metals, are widely applied in various fields of life, such as electricity, machinery, military, medicine and chemical industry (Mudd et al. 2017; Tao et al. 2019). In China, the largest deposit is situated in Sichuan-Guizhou-Yunnan lead zinc triangle, with a distribution of exceeding 400 deposits of varying sizes (Huang et al. 2021). These deposits are mainly buried in karst aquifers. e.g., nearly 60% of the deposits are distributed in aquifers in Yunnan Province (Guo et al. 2013). In the process of mining these deposits, we not only confront the complicated and inconstant geological and hydrogeological conditions, but also bear the threat of various disasters (Ballesteros et al. 2019). Among them, water hazard has been plagued by the safe mining of ore bodies in karst aquifers, causing severe casualties and economic losses (Mahato et al. 2018). Therefore, the risk evaluation of water inrush is an

✉ Wanghua Sui  
suiwanghua@cumt.edu.cn

Qiang Li  
qianglicumt@126.com; tb19010013b4@cumt.edu.cn

Bangtao Sun  
719151317@qq.com

<sup>1</sup> School of Resources and Geosciences, Institute of Mine Water Hazards Prevention and Controlling Technology, China University of Mining and Technology, Xuzhou 221116, China

<sup>2</sup> National Coal Mine Water Hazard Prevention Engineering Technology Research Center, Suzhou 234000, Anhui, China

<sup>3</sup> Yiliang Chihong Mining Co, Ltd, Zhaotong 657600, Yunnan, China

essential segment to reduce the incidence of water disaster accidents and the cost of unnecessary measures in mine safety production.

In terms of the mechanism of water inrush, the formation of water inrush pathways, the main controlling factors of water inrush and water inrush source, the model experiment (Zhang et al. 2017; Yang et al. 2019; Sun et al. 2020), numerical simulation (Golian et al. 2018; Song and Liang 2021), theoretical derivations (Meng et al. 2018; Lin et al. 2020) and geology exploration (Caselle et al. 2020; Wang et al. 2020) were applied to evaluate the risk of water inrush. Among them, the WIC, as a water control standard, was extensively served for the water inrush risk assessment (Li et al. 2018b). However, this method, with less factors considered, cannot satisfy the accurate evaluation of water inrush risk under complicated geological conditions (He et al. 2021).

Recently, various methods considering multi parameters have been added to the water inrush assessment to improve the accuracy of the water inrush risk assessment. Hu et al. (2019) constructed a water inrush prediction model to evaluate the water inrush risk of Qiuji coal mine working face, combining AHP and EWM. Wu et al. (2017) proposed a vulnerability index method combining geographic information system and mathematical method. Li and Sui (2021) presented an improved principal component regression analysis model to analyze the water inrush hazard of the Ordovician karst aquifer. Zhang et al. (2019a) presented a mathematical assessment method for coal floor water inrush risk by integrating the hierarchy variable weight model, indicating a higher accuracy than the variable weight model. Moreover, there are other methods applied to the risk assessment of water inrush, such as evidence theory (Li et al. 2021), TOPSIS method (Shi et al. 2020), set pair analysis (Li et al. 2018a), matter element analysis (Zhang et al. 2019b), and attribute mathematics theory (Xu et al. 2021). Although the above methods have a certain contribution to the evaluation of water inrush, these methods still have their limitations. For example, the calculation steps of the analytic hierarchy process are cumbersome due to repeated construction of judgment matrix for consistency test. In addition, the determined weights, influenced by human, are too subjective. Principal component analysis relies on sample data to extract principal components for quantitative analysis. It cannot realize the transformation between qualitative and quantitative. In addition, the water inrush is characteristic by ambiguity and randomness, affected by multiple factors. It is difficult to simultaneously consider the effects of ambiguity and randomness of water inrush.

In view of the above problems, this paper aims to construct a comprehensive evaluation model for water inrush risk based on IAHP, CRITIC and cloud model. The water inrush evaluation index system was firstly built by

integrating mine multi-source information. Next, the IAHP and CRITIC were applied to determine the subjective weight and objective weight, respectively. The CWM was adopted the combination weights of the evaluation indices. Then, the cloud model was used to calculate the cloud eigenvalue of each evaluation index. The overall water inrush risk level of each sample was determined combined with the weight corresponding to the evaluation index. Finally, the water inrush risk zones of the study area, combined with the water inrush risk level, were divided. Also, the accuracy of the water inrush evaluation model was verified by comparing the actual situation of water inrush. The study can provide a reference for the risk assessment of water inrush of ore body mining in karst aquifer.

## Engineering background

The Maoping lead zinc mine is located in Yiliang County, Zhaotong City, Yunnan Province, China. It is situated in the connecting zone of the Sichuan Basin and the Yunnan-Guizhou Plateau, belonging to the plateau karst erosion mountainous area. The terrain in the mining area is characterized by steep with V-shaped valleys developed. The main drainage, named Luoze River, runs through the mining area from south to north with a drainage datum of around 887 m above sea level (asl). The average annual rainfall of study area is 766.4 mm (Fig. 1). The rainfall is concentrated in June to September, accounting for more than 80% of the annual rainfall.

## Geological conditions

The strata and lithology of the study area from north to south are Upper Permian basalt, Permian limestone, Lower Permian sand shale, Carboniferous limestone, Lower Carboniferous sand shale and Devonian dolomite, respectively. The SMK (Shimenkan) anticline, located in the middle of the study area, runs through the study area in the NNE direction, with a length of 2.3 km. It not only serves as the main ore-controlling structure, but also controls the spatial distribution of the groundwater system in the entire mining area. The strata in the northwest wing of the anticline reversed, with NE trending interlayer fractures developed, resulting in a large-scale ore-bearing and water-storing space. The compressive torsional faults widely distribute in the study area, with multiple sets of faults trending toward the NE to SW, an angle ranging from 40° to 75°.

## Hydrogeological conditions

The underground aquifer in the mining area is affected by the SMK anticline and structures, leading to a  $\Lambda$ -shaped distribution and uneven water yield. The aquifers in the mining area

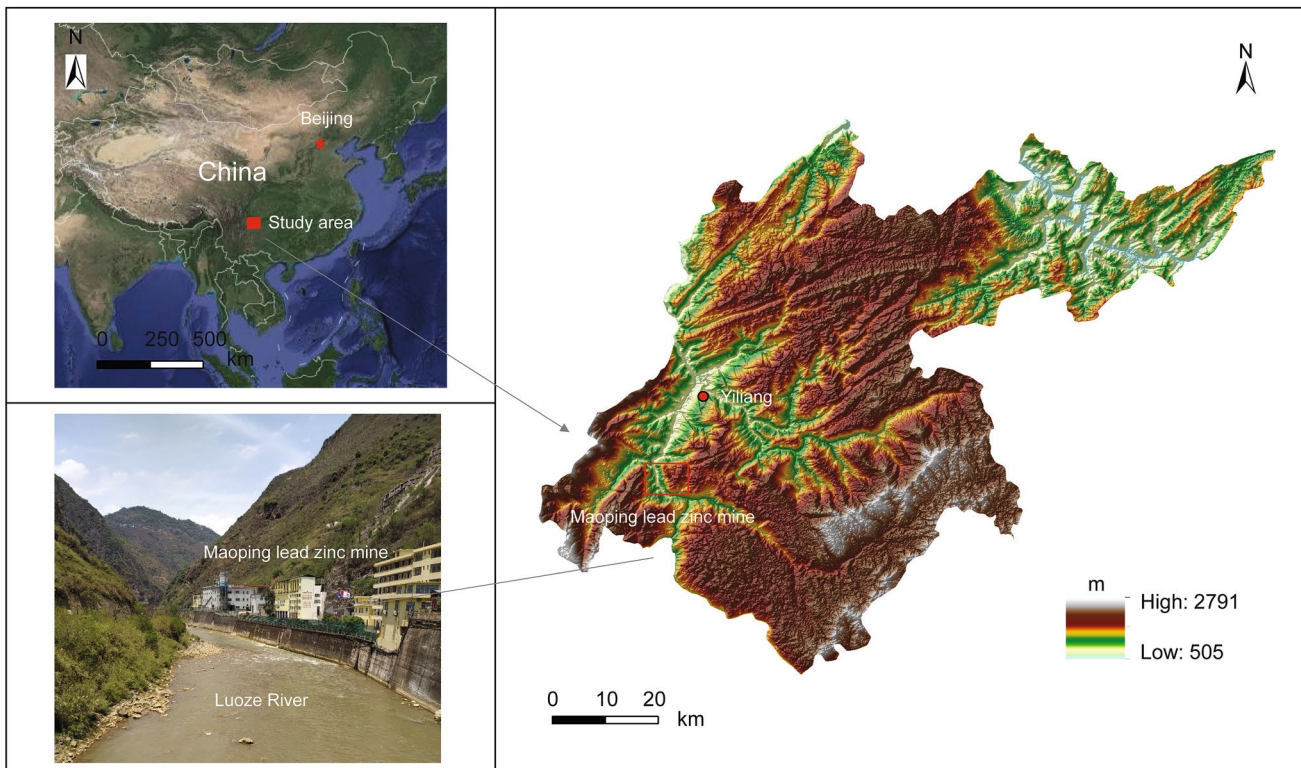


**Fig. 1** The location of the Maoping lead zinc mine

are mainly consisted of Permian Qixia and Maokou Formation karst fissure aquifer, Carboniferous Weining and Fengning Formation karst fissure aquifer, Upper Devonian Zaige Formation karst fissure aquifer, Lower Permian Liangshan Formation structural fissure aquifer and Lower Carboniferous Wanshoushan Formation structural fissure aquifer (Fig. 2). In addition, the average unit inflow of the three karst fissure aquifers is 2.68 L/(s·m), 0.06 L/(s·m), and 0.5 L/(s·m), respectively, indicating a sequence of rich water yield, medium water yield and poor water yield. The structural fissure aquifer of Liangshan Formation and Wanshoushan Formation are regarded as relative aquifers because of poor permeability and water yield. The ore bodies, distributed in the west wing of the SMK anticline, mainly associated with the Carboniferous Weining Formation and the Upper Devonian Zaige Formation.

**Theoretical basis**

The combination of qualitative and quantitative risk assessment techniques is a process involving innovation to ensure the safe mining of ore bodies. In this study, the main steps are as (1) selection of the evaluation indices; (2) determination weights for evaluation indices; (3) construction of water inrush evaluation model.

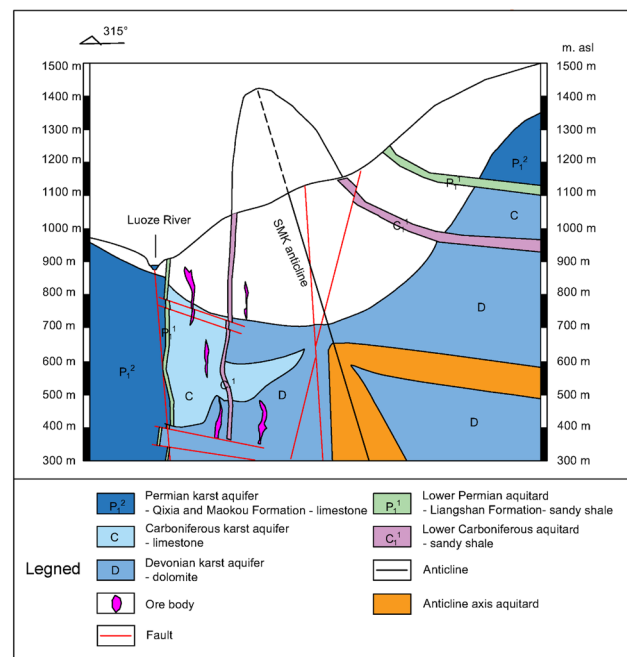


**Fig. 2** Schematic geological and hydrogeological map of study area

## Selection of the evaluation indices

The influencing factors of water inrush, combined with the specific mine water inrush situation, were selected to construct the hierarchical structure. The water inrush risk assessment was taken as the target layer of the hierarchical structure. The factors set, contained in first-grade structure  $B = \{B1, B2, \dots, Bn\}$ , were defined as criterion layer. While the factors set, included in second-grade structure  $C = \{C1, C2, \dots, Cn\}$ , formed index layer (Fig. 3). In addition, the impact of each evaluation factor on the risk of water inrush is different. The main factors affecting risk of water inrush include tectonic conditions, hydrogeological conditions and mining activity. Specifically, fault fractal dimension, drilling fluid consumption, aquifer thickness, water yield, aquifuge thickness, water pressure, mining depth, stop drift length and mining thickness are the second-grade indicators in the hierarchical structure. The tectonic factors not only cut the strata, but also forms water inrush pathways, which are positively correlated with the risk of water inrush. The fault fractal dimension is based on the principle of similarity dimension, representing the complexity of structure by a ratio of quantity change to the change in scale. A large fault fractal dimension value implies a better development of water inrush pathway, with a higher water inrush risk (Adib et al. 2017; Wang and Sui 2022). Hence, the corresponding quantitative indicators are determined by the fault fractal dimension. Drilling fluid consumption is the amount of flushing fluid leakage through strata, reflecting the permeability of the aquifer. The larger the value of drilling fluid consumption is, the better the development and connectivity of formation

fractures are, and the higher the probability of water inrush will be (Yuan et al. 2021; Zhang et al. 2021a). Aquifer thickness and water yield comprise the material basis for aquifer, mirroring the sustainability of water inrush and are positively related to the risk of water inrush (Niu et al. 2020; Liu et al. 2021a). The aquifuge is composed of multiple rock strata with poor water permeability. It has the function of inhibiting water inrush, preventing the water of the aquifer from entering the panel. Thus, the aquifuge thickness was defined as a negative correlation factor (Zhang et al. 2021b). The water pressure, positively correlated with the risk of water inrush, determines whether water inrush occurs, reflecting the severity of water inrush (Duan and Zhao 2021; Wang et al. 2022). The mining depth, stop drift length and mining thickness are related to the destruction of the surrounding rock of the ore body, which indicates the rule whereby the higher its value is, the higher the possibility of water inrush. The overburden fissures extend to the aquifer, leading to the occurrence of water inrush (Liu et al. 2021b; Li et al. 2022). Also, the water inrush risk of these 9 factors was classified into five levels, i.e., very low (I), low (II), medium (III), high (IV), and very high (V), on the basis of the mine measured data (Table 1).

## Determination weights for evaluation indices

### IAHP

The AHP, a practical multi-criteria decision-making method, was proposed by Saaty (Saaty 1980). This method uses an orderly hierarchical structure to represent complex problems

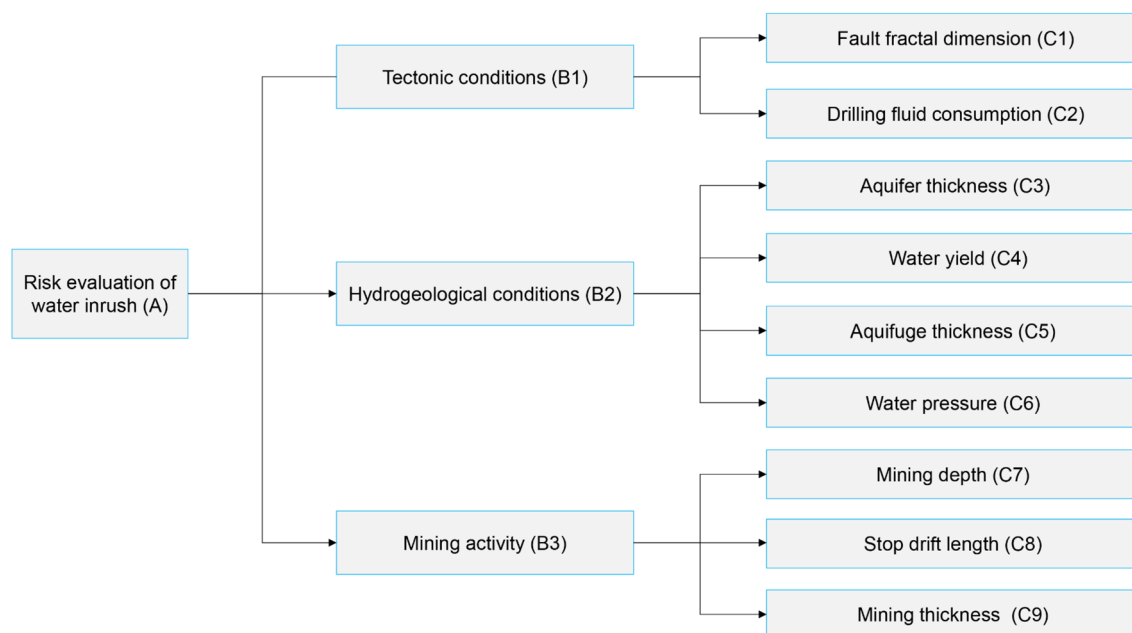


Fig. 3 Hierarchical structure of evaluation index

**Table 1** Values and grading of indices affecting the risk of water inrush

Evaluation index			Risk level of water inrush				
First grade	Second grade	Measured value	I	II	III	IV	V
B1	C1	0.65~5.63	0.65–1.50	1.51–3.00	3.01–3.80	3.81–4.50	4.51–5.63
	C2 (m <sup>3</sup> /h)	0.15~4.55	0.15–1.00	1.01–2.80	2.81–3.50	3.51–4.00	4.01–4.55
B2	C3 (m)	55~220	55–85	86–120	121–150	151–180	181–220
	C4 (L/(s·m))	0.01~1.68	0.01–0.15	0.16–0.30	0.31–0.75	0.76–1.50	1.51–1.68
	C5 (m)	16.50~65.84	60.01–65.84	50.01–60.00	35.01–50.00	20.01–35.00	16.50–20.00
B3	C6 (Mpa)	0.15~3.20	0.15–0.60	0.61–1.20	1.21–1.80	1.81–3.00	3.01–3.20
	C7 (m)	670~430	651–670	601–650	551–600	451–550	430–450
	C8 (m)	0~60	0–15	16–25	26–30	31–50	51–60
	C9 (m)	0~6.0	0–2.5	2.6–3.0	3.1–3.5	3.6–4.5	4.6–6.0

with qualitatively and quantitatively evaluate index weights. The IAHP adopts the three-scale method to construct the judgment matrix without the tedious step of consistency check (Wang et al. 2019b). It is more convenient than the AHP method with traditional nine-scale method. The specific steps are as follows:

*Establish a multilevel hierarchy structure.* The decision-making system was divided into several hierarchical levels including objective level, criterion level and decision level, respectively. We classified the main evaluation indices of water inrush into three levels in this study.

*Construct the comparison matrices.* According to the relative importance of the evaluation indices, the three-scale (0, 1 and 2) method was adopted to construct the comparison matrix  $D$  at different levels. Among them, 0 presents that the importance of  $i$  is less than  $j$ ; 1 declares that the importance of  $i$  is equal to  $j$ ; 2 indicates that the importance of  $i$  is large than  $j$ . Also, the judgment matrix  $E = (e_{ij})_{n \times n}$  is calculated by the following formula.

$$e_{ij} = \begin{cases} d_i - d_j & d_i > d_j \\ 1 & d_i = d_j \\ 1/(d_j - d_i) & d_i < d_j \end{cases} \quad (1)$$

Where  $d_i$  and  $d_j$  are the row sum of comparison matrix  $D$ .

*Determine the subject weights.* The weight of the main evaluation indices was calculated by following formula:

$$\alpha_j = \frac{\sqrt[n]{\prod_{i=1}^n e_{ij}}}{\sum_{i=1}^n \sqrt[n]{\prod_{i=1}^n e_{ij}}} \quad (2)$$

Where  $\alpha_j$  is the subject weight of the  $j$ th evaluation index.

## CRITIC

The CRITIC, firstly proposed by Diakoulaki et al. (1995), is a more scientific objective weighting method. This method determines the index weight according to the contrast intensity and conflict between the evaluation indices. Meanwhile, it considers the difference and correlation between the indices. The calculation steps are as follows.

*Standardization of evaluation indices.* According to the effect of evaluation index on water inrush, the standardized equations are classified into positive correlation and negative correlation.

$$X_{ji} = \frac{x_{ji} - \min(x_{ji})}{\max(x_{ji}) - \min(x_{ji})} \quad (3)$$

$$X_{ji} = \frac{\max(x_{ji}) - x_{ji}}{\max(x_{ji}) - \min(x_{ji})} \quad (4)$$

where  $X_{ji}$  is the standardized data;  $x_{ji}$  is the original data;  $\min(x_{ji})$  and  $\max(x_{ji})$  are the minimum and maximum values of each evaluation index, respectively.

*Calculation of standard deviation and correlation coefficient.* In CRITIC, the standard deviation and correlation coefficient are applied to represent the difference and conflict between indicators, respectively. The larger the standard deviation, the greater the difference between the indicators. A positive correlation coefficient indicates that the conflict between the indicators is smaller. The standard and correlation coefficients between indicators are calculated as follows:

$$S_j = \sqrt{\frac{\sum_{i=1}^m (X_{ji} - \bar{X}_j)^2}{m-1}} \quad (5)$$

$$r_{kl} = \frac{\sum_{i=1}^m (X_{ik} - \bar{X}_k)(X_{il} - \bar{X}_l)}{\sqrt{\sum_{i=1}^m (X_{ik} - \bar{X}_k)^2 \sum_{i=1}^m (X_{il} - \bar{X}_l)^2}} \tag{6}$$

where  $S_j$  is the standard deviation of  $j$ th evaluation indices;  $\bar{X}_j$  is the mean value of  $j$ th evaluation indices;  $r_{kl}$  is the correlation coefficient between evaluation indices,  $k = 1, 2, \dots, n$ ;  $l = 1, 2, \dots, k$ . Therefore, we can construct the correlation coefficient matrix  $R = (r_{ij})_{n \times n}$  of the evaluation index.

**Determination of indices conflict.** The conflict between evaluation indices is calculated as follows:

$$R_j = \sum_{k=1}^n (1 - r_{kl}) \tag{7}$$

where  $R_j$  is the conflict of the  $j$ th evaluation index.

**Calculation of evaluation index information amount and object weight.** The information amount and weight of the evaluation index are determined by Eq. (8) and Eq. (9), respectively.

$$t_j = S_j R_j = \sum_{i=1}^n (1 - r_{ij}) \sqrt{\frac{\sum_{i=1}^n (X_i - \bar{X}_i)^2}{n - 1}} \tag{8}$$

$$\beta_j = \frac{t_j}{\sum_{j=1}^n t_j} \tag{9}$$

where  $t_j$  is the information amount of  $j$ th evaluation index;  $\beta_j$  is the object weight of  $j$ th evaluation index.

### Determination of combination weight

To make the combination weight as close as possible to the subjective weight and the objective weight, the objective function of the combination weight is constructed by combining the concept of Kullback information (Thiesen et al. 2019), avoiding leaning toward either side. Also, the combination weight of the evaluation index can be obtained using the Lagrange multiplier method.

$$\left\{ \begin{array}{l} \min J(w) = \sum_{j=1}^n (w_j \ln \frac{w_j}{\alpha_j} + w_i \ln \frac{w_j}{\beta_j}) \\ \text{s.t. } \sum_{j=1}^n w_j = 1, w_j \geq 0, i = 1, 2, \dots, n \end{array} \right\} \tag{10}$$

$$w_j = \frac{\sqrt{\alpha_j \beta_j}}{\sum_{j=1}^n \sqrt{\alpha_j \beta_j}} \tag{11}$$

where  $w_j$  is the combination weight of the  $j$ th evaluation index.

## Construction of water inrush evaluation model

### Definition of cloud

The cloud model represents the uncertainty transformation between concept and its quantitative representation through digital features to realize the qualitative and quantitative transformation (Wu et al. 2021). Supposed  $V$  is a qualitative concept in the quantitative domain  $U$ ,  $x \in V$  represents a random realization on  $U$ , indicating the certainty degree of  $x$  to  $U$  as  $\mu(x) \in [0, 1]$ . The distribute of  $x$  on  $V$  forms a cloud  $\mu(x)$ . Furthermore, each  $x$  was called a cloud droplet. The digital features of cloud model are composed of three eigenvalues i.e., expectation ( $Ex$ ), entropy ( $En$ ) and hyperentropy ( $He$ ). Among them, The  $Ex$  presents the median value of the quantitative domain  $U$ . The  $En$  reflects the numerical range of the quantitative domain  $U$ . The  $He$  means the degree of dispersion of cloud droplets under a certain certainty degree. The conversion between eigenvalues and certainty degree (Eq. (12)) was realized through cloud generator (Wang et al. 2019a).

$$\mu(x) = \exp \left[ -\frac{(x - Ex)^2}{2En^2} \right] \tag{12}$$

### Calculation of standard cloud

Particularly, the qualitative description of each risk evaluation index is converted into quantitative characteristic values by the normal cloud generator. Conversely, the transformation of quantitative values to qualitative concepts is achieved using the backward cloud generator. Three eigenvalues of the cloud model were determined on the basis of the specific evaluation criteria. For a boundary of the form  $[x_{i\min}, x_{i\max}]$ , the eigenvalues were calculated by the cloud model transformation models.

$$\left\{ \begin{array}{l} Ex = (x_{i\min} + x_{i\max})/2 \\ En = (x_{i\max} - x_{i\min})/6 \\ He = k \end{array} \right. \tag{13}$$

### Comprehensive assessment of water inrush risk

Combined with the standard cloud eigenvalues of the evaluation indices, the certainty of the actual samples corresponding to different risk levels is calculated by Eq. (12). In addition, combined with the weights of the evaluation indicators, the comprehensive certainty corresponding to the different risk levels of each sample is determined by Eq. (14). The water inrush level of each sample is defined according to the principle of maximum certainty.

$$U_i = \sum_{j=1}^n \mu(x_{ij})w_j \tag{14}$$

where  $U_i$  is the comprehensive certainty of the  $i$ th sample;  $\mu(x_i)$  is the standard cloud certainty of  $j$ th evaluation index;  $w_j$  is the weight of  $j$ th evaluation index,  $j=1, 2, \dots, n$ .

### Results and analysis

#### Calculation and results of IAHP

The comparison matrix corresponding to each grade was calculated by comparing the relative importance of indicators under different grade structures.

$$D_{A-B1,2,3} = \begin{pmatrix} 1 & 2 & 2 \\ 0 & 1 & 2 \\ 0 & 0 & 1 \end{pmatrix} \tag{15}$$

$$D_{B1-C1,2} = \begin{pmatrix} 1 & 2 \\ 0 & 1 \end{pmatrix} \tag{16}$$

$$D_{B2-C3,4,5,6} = \begin{pmatrix} 1 & 0 & 0 & 0 \\ 2 & 1 & 2 & 2 \\ 2 & 0 & 1 & 2 \\ 1 & 0 & 0 & 1 \end{pmatrix} \tag{17}$$

$$D_{B3-C7,8,9} = \begin{pmatrix} 1 & 0 & 2 \\ 2 & 1 & 2 \\ 0 & 0 & 1 \end{pmatrix} \tag{18}$$

The judgment matrix at different grades was obtained by Eq. (1).

$$E_{A-B1,2,3} = \begin{pmatrix} 1 & 2 & 4 \\ 1/2 & 1 & 2 \\ 1/4 & 1/2 & 1 \end{pmatrix} \tag{19}$$

$$E_{B1-C1,2} = \begin{pmatrix} 1 & 2 \\ 1/2 & 1 \end{pmatrix} \tag{20}$$

$$E_{B2-C3,4,5,6} = \begin{pmatrix} 1 & 1/6 & 1/4 & 1/2 \\ 6 & 1 & 2 & 4 \\ 4 & 1/2 & 1 & 2 \\ 2 & 1/4 & 1/2 & 1 \end{pmatrix} \tag{21}$$

$$E_{B3-C7,8,9} = \begin{pmatrix} 1 & 1/2 & 2 \\ 2 & 1 & 4 \\ 1/2 & 1/4 & 1 \end{pmatrix} \tag{22}$$

The weights of evaluation indices under different hierarchical structures were determined by application of Eq. (2). Additionally, we obtained the subjective weight of each evaluation index corresponding to the overall goal as  $\alpha=(0.38, 0.19, 0.02, 0.15, 0.08, 0.04, 0.04, 0.08, 0.02)^T$ .

#### Calculation and results of CRITIC

Combined with the correlation between the evaluation index and water inrush, the standardized value of each evaluation index was calculated by Eqs. (3) and (4), as shown in the Table 2.

The corresponding correlation coefficient matrix was constructed due to the result of correlation coefficient between the evaluation indicators calculated by Eq. (6).

$$R = \begin{pmatrix} 1 & 0.90 & 0.44 & 0.19 & -0.19 & -0.49 & 0.49 & 0.44 & 0.43 \\ 0.90 & 1 & 0.21 & 0.39 & 0.04 & -0.41 & 0.41 & 0.39 & 0.42 \\ 0.44 & 0.21 & 1 & -0.61 & -0.75 & -0.41 & 0.41 & 0.10 & -0.02 \\ 0.19 & 0.39 & -0.61 & 1 & 0.61 & 0.34 & -0.34 & -0.02 & 0.15 \\ -0.19 & 0.04 & -0.75 & 0.61 & 1 & 0.37 & -0.37 & -0.24 & -0.13 \\ -0.49 & -0.41 & -0.41 & 0.34 & 0.37 & 1 & -1 & -0.48 & -0.34 \\ 0.49 & 0.41 & 0.41 & -0.34 & -0.37 & -1 & 1 & 0.48 & 0.34 \\ 0.44 & 0.39 & 0.10 & -0.02 & -0.24 & -0.48 & 0.48 & 1 & 0.97 \\ 0.43 & 0.42 & -0.02 & 0.15 & -0.13 & -0.34 & 0.34 & 0.97 & 1 \end{pmatrix} \tag{23}$$

The information amount and objective weight of the evaluation index were determined by Eq. (8) and Eq. (9), respectively, i.e.,  $t=(1.92, 1.75, 2.68, 2.51, 2.84, 3.82, 2.78, 2.37, 2.29)^T$  and  $\beta=(0.08, 0.08, 0.12, 0.11, 0.12, 0.17, 0.12, 0.10, 0.10)^T$ .

#### Determination of combination weight

Combined with the subjective weight and objective weight of the evaluation index, the combined weight of each evaluation index was obtained by Eq. (11), i.e.,  $w=(0.21, 0.14, 0.06, 0.15, 0.12, 0.09, 0.08, 0.11, 0.05)^T$ .

**Table 2** Standardized value of each evaluation index

Samples	C1	C2	C3	C4	C5	C6	C7	C8	C9
ZK01	0.64	0.59	0.03	0.92	0.83	1.00	0.00	0.33	0.50
ZK02	0.74	0.65	0.24	0.50	0.92	0.25	0.75	0.50	0.70
ZK03	0.50	0.67	0	0.98	0.88	1	0	0.40	0.58
ZK04	0.83	0.93	0.48	0.44	0.76	0.75	0.25	0.53	0.58
ZK05	1	1.00	0.58	0.47	0.81	0.29	0.71	0	0
ZK06	0.92	0.80	0.67	0.50	0	0.00	1	0.85	0.83
ZK07	0.93	0.77	0.88	0	0.09	0.25	0.75	0.95	1
ZK08	0.86	0.61	0.64	0.08	0.15	0.00	1	1	0.92
ZK09	0.96	0.89	1	0.26	0.12	0.25	0.75	0	0
ZK10	0.65	0.60	0.45	0.14	0.44	0.15	0.85	0	0
ZK11	0.12	0	0.61	0.02	0.32	0.75	0.25	0	0
ZK12	0	0.02	0.04	0.11	0.56	0.75	0.25	0	0
ZK13	0.26	0.60	0.21	0.17	0.64	0	1	0.70	0.68
ZK14	0.10	0.05	0.64	0.07	0.60	0.75	0.25	0	0
ZK15	0.85	0.65	0.52	0.15	0.71	0.00	1	0.77	0.58
ZK16	0.62	0.70	0.06	1	1	0.25	0.75	0.37	0.42

### Determination of evaluation indices standard cloud

Considering the water inrush risk classification of each evaluation index (Table 1), the standard cloud feature values corresponding to different risk levels of the evaluation index was calculated to obtain the corresponding standard cloud distribution (Fig. 4).

### Water inrush risk assessment

Combined with the standard cloud eigenvalues of the water inrush evaluation index, the certainty of the sample under different risk levels was calculated by Eq. (12). The overall certainty of the sample, also, was obtained by Eq. (14), combined with the weight value corresponding to the evaluation index. In addition, the water inrush risk level of the sample was determined according to the principle of maximum certainty, as shown in the Table 3.

To more intuitively reflect the risk zone of water inrush in the study area, combined with the water inrush risk levels corresponding to each sample, the distribution of water inrush risk corresponding to different levels (Fig. 5) was determined with GIS.

Figure 5(a) shows that the water inrush risk in the study area is classified into five levels, i.e., risk level I, risk level II, risk level III, risk level IV and risk level V. The risk level of water inrush from north to south in the study area changes from high to low. Among them, the areas with risk level V are mainly distributed in the north of the study area, implying a higher probability of water inrush. The main reason is that this area is adjacent to the Permian Qixia and Maokou strong water-rich aquifers. Furthermore, the strata in this area is relatively fragmented under the action of fault

cutting, resulting in a high probability of water inrush during the mining process. The areas with risk level I are mainly distributed in the middle of the study area, indicating a lower probability of water inrush, due to the weak water yield of the strata and the barrier effect of the relative aquifer.

### Discussions

#### Comparative verification

To verify the CWM water inrush prediction model, the water inrush prediction results of IAHP, CRITIC and WIC were carried out (Table 3), and corresponding water inrush risk areas were defined (Fig. 6).

Figure 6(a) shows that the water inrush risk area is also divided into five areas with IAHP. The risk level V areas are mainly distributed in the north of the study area, and the risk level I areas are mainly located in the middle of the study area. Among the four water inrush points, the TS04 is located in the area of water inrush risk level I. The remaining water inrush points are located in the areas of risk level IV and risk level V.

As shown in Fig. 6(b), the area with risk level V is distributed in the north of the study area, and the area with risk level I is located in the east of the study area, according to the CRITIC. Also, three water inrush points are located in the area of risk level IV, and one water inrush point is located in the area of risk level V. According to “Safety Technical Specifications for Water Prevention and Control in Metal and Nonmetal Underground Mines” (Ministry of Emergency Management of the People’s Republic of China 2018), the WIC in the tectonic development area is 0.06 MPa/m as



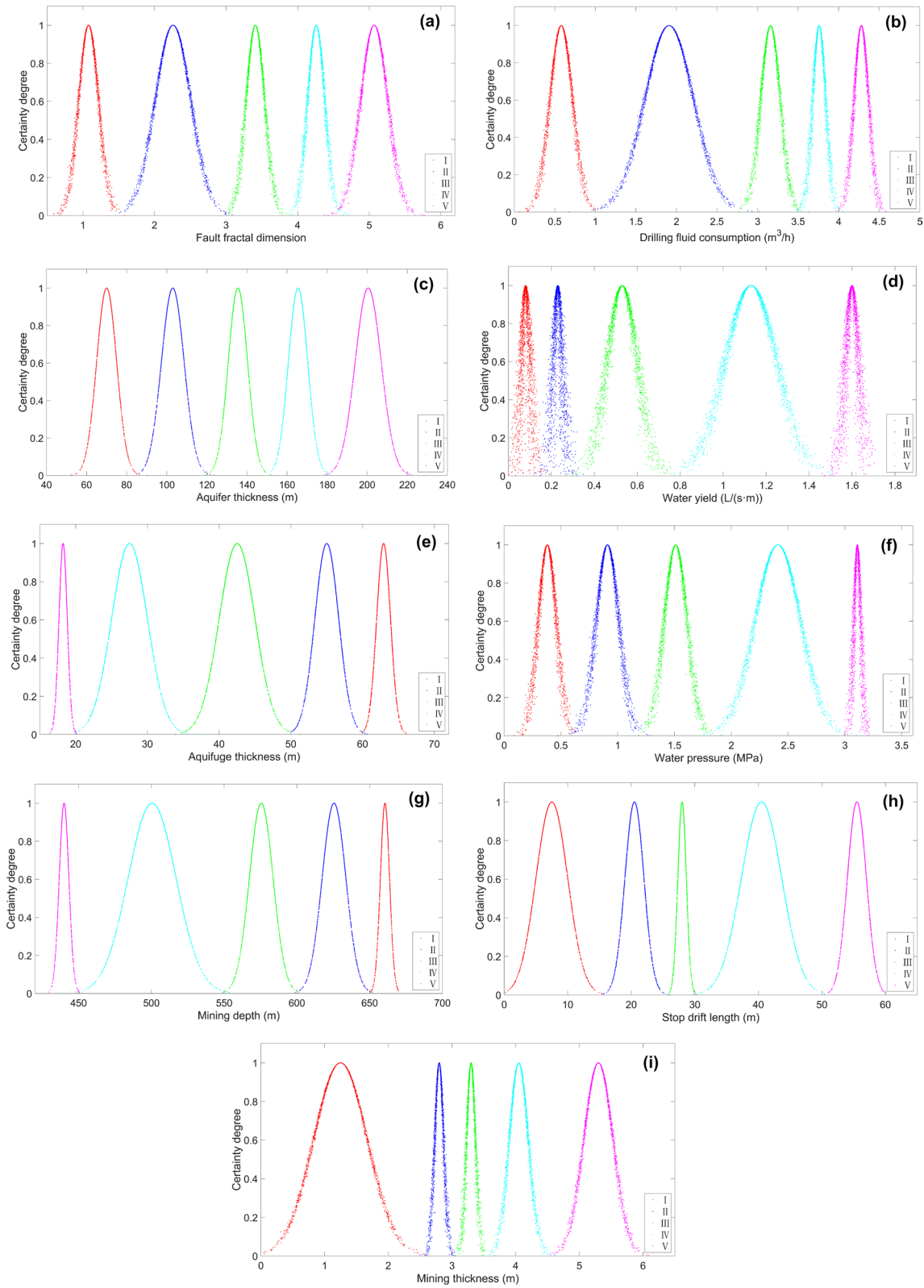
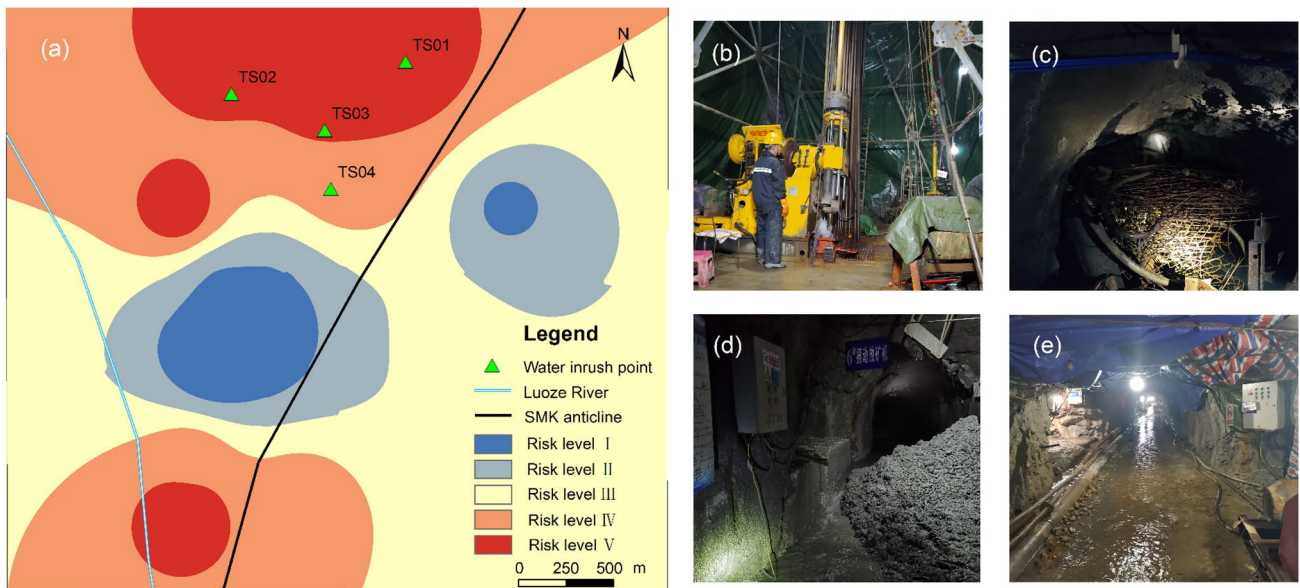


Fig. 4 Evaluation index standard cloud distribution

**Table 3** Classification of water inrush risk levels of samples

Samples	Overall certainty of different levels in CM					Water inrush risk level of different methods			
	I	II	III	IV	V	CWM	IAHP	CRITIC	WIC
ZK01	0.01	0.11	0.00	0.08	0.06	II	II	II	I
ZK02	0.00	0.11	0.09	0.16	0.00	IV	IV	IV	V
ZK03	0.00	0.02	0.19	0.01	0.04	III	III	III	V
ZK04	0.00	0.01	0.06	0.20	0.21	V	V	IV	V
ZK05	0.00	0.03	0.00	0.18	0.01	IV	IV	IV	I
ZK06	0.00	0.00	0.00	0.13	0.18	V	V	IV	I
ZK07	0.03	0.09	0.00	0.08	0.26	V	V	V	I
ZK08	0.00	0.01	0.01	0.03	0.19	V	V	V	I
ZK09	0.00	0.09	0.08	0.07	0.05	II	V	II	I
ZK10	0.00	0.06	0.13	0.02	0.00	III	III	III	I
ZK11	0.17	0.01	0.00	0.10	0.00	I	I	IV	V
ZK12	0.03	0.05	0.02	0.09	0.00	IV	II	IV	V
ZK13	0.00	0.14	0.01	0.15	0.00	IV	II	IV	I
ZK14	0.23	0.01	0.00	0.12	0.00	I	I	IV	V
ZK15	0.00	0.02	0.11	0.07	0.13	V	V	III	I
ZK16	0.04	0.16	0.11	0.07	0.01	II	III	II	V



**Fig. 5** Risk zoning map of water inrush in the study area

the critical value to judge whether the water inrush occurs or not. Figure 6(c) shows that the study area is only divided into the areas of risk level I ( $WIC \leq 0.06$  MPa/m) and the area of risk level V ( $WIC > 0.06$  MPa/m). Among them, the area of risk level I is much larger than the area of risk level V, indicating a fuzzy division of water inrush risk zones. Only one of the four water inrush points, moreover, is located in

area of risk level V, and the rest are in area of risk level I. It is inconsistent with the actual water inrush situation.

By comparing the division of water inrush risk areas and the fitting of water inrush points for the three methods, it can be concluded that the water inrush risk prediction accuracy is ranked as  $CWM > CRITIC > IAHP > WIC$ . The CWM not only reflects subjective experience, but also retains objective original

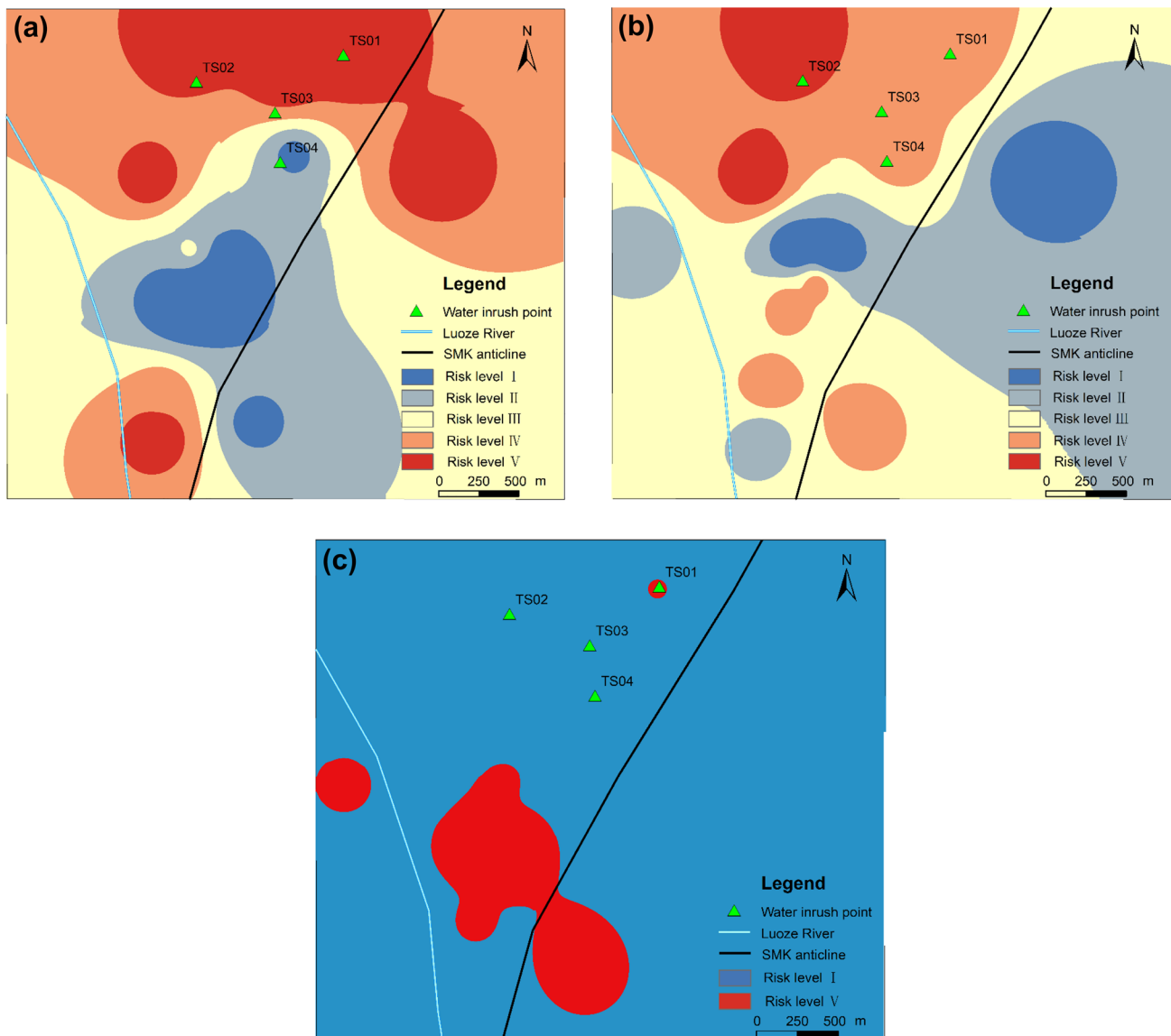


**Fig. 6** Risk zoning map of water inrush with IAHP, CRITIC and WIC

data information. It is suitable for practical engineering applications, playing a guiding role in water hazard prevention.

### Site construction verification

Figure 5 shows that there are 4 water inrush points, namely, TS01, TS02, TS03 and TS04, distributed in the area of level IV and V in the north of the study area. TS01 occurred during the prospecting process in the 670 m middle section (Fig. 5(b)), with a water yield of  $5.25 \text{ m}^3/\text{h}$ . TS02 was located in the No. 2 ore belt in the 610 m middle section (Fig. 5(c)) with a water yield of  $20.10 \text{ m}^3/\text{h}$ . TS03 was the drain hole of No. 2 ore belt in the 610 m middle section (Fig. 5(d)), with a water yield of  $10.05 \text{ m}^3/\text{h}$ . TS04 occurred

in the tunnel excavation process in the 490 m middle section (Fig. 5(e)) with a water yield of  $22.50 \text{ m}^3/\text{h}$ . According to the maximum probability criterion, the water inrush points were distributed in areas with high water inrush probability. It can be found that the fitting effect with the on-site water inrush points can reach an accuracy of more than 90%.

### Conclusion

A comprehensive cloud water inrush evaluation model was proposed to evaluate the water inrush from the karst aquifer in Maoping lead zinc mine. The major findings are as follows:

Comprehensively considering the tectonic conditions, hydrogeological conditions and mining activity of the study area, 9 influencing factors were selected as the indices of water inrush evaluation, i.e., fault fractal dimension, drilling fluid consumption, aquifer thickness, water yield, aquifuge thickness, water pressure, mining depth, stop drift length and mining thickness.

The IAHP was applied to improve the calculation efficiency of the subjective weight of the water inrush evaluation index. The original information of the evaluation index was preserved by the CRITIC, improving the calculation accuracy of the objective weight of the evaluation index. The combined weight constructed by the concept of Kullback information, avoiding the bias of the weight. It has the advantages of both subjective and objective weights.

The water inrush evaluation model based on the cloud model can realize the qualitative and quantitative conversion between evaluation indices. The water inrush risk level area divided by the CWM water inrush prediction model have a good fitting effect with the actual, with an accuracy of 90%. Comparing the IAHP and the CRITIC, its prediction accuracy is higher than both. This method plays a guiding role in mine mining planning and water hazard prevention.

**Author contributions** All authors contributed to the study conception and design. Material preparation, data collection and analysis were performed by QL and BS. The first draft of the manuscript was written by WS and all authors commented on previous versions of the manuscript. All authors read and approved the final manuscript.

**Funding** This work was supported by National Natural Science Foundation of China under Grant No. 42130706.

**Data availability** All data analyzed during the study are included in the submitted article.

## Declarations

**Conflict of interest** The authors have no relevant financial or non-financial interests to disclose.

## References

- Adib A, Afzal P, Ilani SM, Aliyari F (2017) Determination of the relationship between major fault and zinc mineralization using fractal modeling in the Behabad fault zone, central Iran. *J Afr Earth Sci* 134:308–319. <https://doi.org/10.1016/j.jafrearsci.2017.06.025>
- Ballesteros D, Giral S, García-Sansegundo J, Jiméñez-Sánchez M, (2019) Quaternary regional evolution based on karst cave geomorphology in Picos de Europa (Atlantic Margin of the Iberian Peninsula). *Geomorphol* 336:133–151. <https://doi.org/10.1016/j.geomorph.2019.04.002>
- Caselle C, Bonetto S, Comina C, Stocco S (2020) GPR surveys for the prevention of karst risk in underground gypsum quarries. *Tunnelling Undergr Space Techno* 95:103137. <https://doi.org/10.1016/j.tust.2019.103137>
- Diakoulaki D, Mavrotas G, Papayannakis L (1995) Determining objective weights in multiple criteria problems: the critic method. *Comput Oper Res* 22:763–770. [https://doi.org/10.1016/0305-0548\(94\)00059-H](https://doi.org/10.1016/0305-0548(94)00059-H)
- Duan HF, Zhao LJ (2021) New evaluation and prediction method to determine the risk of water inrush from mining coal seam floor. *Environ Earth Sci* 80:30. <https://doi.org/10.1007/s12665-020-09339-y>
- Golian M, Teshnizi ES, Nakhaei M (2018) Prediction of water inflow to mechanized tunnels during tunnel-boring-machine advance using numerical simulation. *Hydrogeol J* 26:2827–2851. <https://doi.org/10.1007/s10040-018-1835-x>
- Guo F, Jiang G, Yuan D, Polk JS (2013) Evolution of major environmental geological problems in karst areas of Southwestern China. *Environ Earth Sci* 69(7):2427–2435. <https://doi.org/10.1007/s12665-012-2070-8>
- He JH, Li WP, Qiao W, Yang Z, Wang QQ (2021) Risk assessment of water inrushes from bed separations in Cretaceous strata corresponding to different excavation lengths during mining in the Ordos Basin. *Geomatics Nat Hazards Risk* 12(1):2300–2327. <https://doi.org/10.1080/19475705.2021.1950220>
- Hu YB, Li WP, Wang QQ, Liu SL, Wang ZK (2019) Evaluation of water inrush risk from coal seam floors with an AHP–EWM algorithm and GIS. *Environ Earth Sci* 78:290. <https://doi.org/10.1007/s12665-019-8301-5>
- Huang H, Chen ZH, Wang T, Zhang L, Liu TW, Zhou GM (2021) Pattern and degree of groundwater recharge from river leakage in a karst canyon area under intensive mine dewatering. *Sci Total Environ* 774:144921. <https://doi.org/10.1016/j.scitotenv.2020.144921>
- Li B, Wu Q, Duan XQ, Chen MY (2018a) Risk analysis model of water inrush through the seam floor based on set pair analysis. *Mine Water Environ* 37:281–287. <https://doi.org/10.1007/s10230-017-0498-5>
- Li B, Zhang WP, Long J, Fan J, Chen MY, Li T, Liu P (2022) Multi-source information fusion technology for risk assessment of water inrush from coal floor karst aquifer. *Geomat Nat Hazards Risk* 13(1):2086–2106. <https://doi.org/10.1080/19475705.2022.2108728>
- Li Q, Sui WH (2021) Risk evaluation of mine-water inrush based on principal component logistic regression analysis and an improved analytic hierarchy process. *Hydrogeol J* 29:1299–1311. <https://doi.org/10.1007/s10040-021-02305-3>
- Li SC, Liu C, Zhou ZQ, Li LP, Shi SS (2021) Multi-sources information fusion analysis of water inrush disaster in tunnels based on improved theory of evidence. *Tunnelling Undergr Space Techno* 113:103948. <https://doi.org/10.1016/j.tust.2021.103948>
- Li WP, Liu Y, Qiao W, Zhao CX, Yang DD, Guo QC (2018b) An improved vulnerability assessment model for floor water bursting from a confined aquifer based on the water inrush coefficient method. *Mine Water Environ* 37:196–204. <https://doi.org/10.1007/s10230-017-0463-3>
- Lin M, Dong SN, Zhou WF, Wang W, Li A, Shi ZY (2020) Data analysis and key parameters of typical water hazard control engineering in coal mines of China. *Mine Water Environ* 39:331–344. <https://doi.org/10.1007/s10230-020-00684-9>
- Liu JW, Yang BB, Yuan SC, Li ZH, Yang MF, Duan LH (2021a) A fuzzy analytical process to assess the risk of disaster when backfill mining under aquifers and buildings. *Mine Water Environ* 40:891–901. <https://doi.org/10.1007/s10230-021-00822-x>
- Liu WT, Han MK, Meng XX, Qin YY (2021b) Mine water inrush risk assessment evaluation based on the GIS and combination weight-cloud model: a case study. *ACS Omega* 6(48):32671–32681. <https://doi.org/10.1021/acsomega.1c04357>
- Mahato MK, Singh PK, Singh AK, Tiwari AK (2018) Assessment of hydrogeochemical processes and mine water suitability for

- domestic, irrigation, and industrial purposes in east Bokaro coal-field, India. *Mine Water Environ* 37:493–504. <https://doi.org/10.1007/s10230-017-0508-7>
- Meng XX, Liu WT, Mu DR (2018) Influence analysis of mining's effect on failure characteristics of a coal seam floor with faults: a numerical simulation case study in the Zhaolou coal mine. *Mine Water Environ* 37:754–762. <https://doi.org/10.1007/s10230-018-0532-2>
- Ministry of Emergency Management of the People's Republic of China (2018) Safety technical specifications for water prevention and control in metal and nonmetal underground mines. China Coal Industry Publishing House, Beijing
- Mudd GM, Jowitt SM, Werner TT (2017) The world's lead-zinc mineral resources: scarcity, data, issues and opportunities. *Ore Geol Rev* 80:1160–1190. <https://doi.org/10.1016/j.oregeorev.2016.08.010>
- Niu HG, Wei JC, Yin HY, Xie DL, Zhang WJ (2020) An improved model to predict the water-inrush risk from an Ordovician limestone aquifer under coal seams: a case study of the Longgu coal mine in China. *Carbonates Evaporites* 35:73. <https://doi.org/10.1007/s13146-020-00590-9>
- Saaty TL (1980) The analytic hierarchy process: planning, priority setting, resource allocation. McGraw-Hill, New York
- Shi LQ, Qiu M, Teng C, Wang Y, Liu TH, Qu XY (2020) Risk assessment of water inrush to coal seams from underlying aquifer by an innovative combination of the TFN-AHP and TOPSIS techniques. *Arab J Geosci* 13:600. <https://doi.org/10.1007/s12517-020-05588-0>
- Song WC, Liang ZZ (2021) Theoretical and numerical investigations on mining-induced fault activation and groundwater outburst of coal seam floor. *Bull Eng Geol Environ* 80:5757–5768. <https://doi.org/10.1007/s10064-021-02245-y>
- Sun Q, Meng GH, Sun K, Zhang JX (2020) Physical simulation experiment on prevention and control of water inrush disaster by back-filling mining under aquifer. *Environ Earth Sci* 79:429. <https://doi.org/10.1007/s12665-020-09174-1>
- Tao M, Zhang X, Wang SF, Guo WZ, Jaing Y (2019) Life cycle assessment on lead-zinc ore mining and beneficiation in China. *J Cleaner Prod* 237:117833. <https://doi.org/10.1016/j.jclepro.2019.117833>
- Thiesen S, Darscheid P, Ehret U (2019) Identifying rainfall-runoff events in discharge time series: a data-driven method based on information theory. *Hydrol Earth Syst Sci* 23:1015–1034. <https://doi.org/10.5194/hess-23-1015-2019>
- Wang DD, Sui WH (2022) Hydrogeological effects of fault geometry for analysing groundwater inflow in a coal mine. *Mine Water Environ* 41:93–102. <https://doi.org/10.1007/s10230-021-00795-x>
- Wang XT, Li SC, Xu ZH, Hu J, Pan DD, Xue YG (2019a) Risk assessment of water inrush in karst tunnels excavation based on normal cloud model. *Bull Eng Geol Environ* 78:3783–3798. <https://doi.org/10.1007/s10064-018-1294-6>
- Wang XY, Yao MJ, Zhang JG, Zhao W, Huang PH, Guo JW, Chen GS, Zhang B (2019b) Evaluation of water bursting in coal seam floor based on improved AHP and fuzzy variable set theory. *J Min Safe Eng* 36(3):558–565
- Wang Y, Shi LQ, Wang M, Liu TH (2020) Hydrochemical analysis and discrimination of mine water source of the Jiaojia gold mine area. *China Environ Earth Sci* 79:123. <https://doi.org/10.1007/s12665-020-8856-1>
- Wang YC, Chen F, Sui WH, Meng FS, Geng F (2022) Large-scale model test for studying the water inrush during tunnel excavation in fault. *Bull Eng Geol Environ* 81:238. <https://doi.org/10.1007/s10064-022-02733-9>
- Wu Q, Guo XM, Shen JJ, Xu S, Liu SQ, Zeng YF (2017) Risk assessment of water inrush from aquifers underlying the Gushuyuan coal mine, China. *Mine Water Environ* 36:96–103. <https://doi.org/10.1007/s10230-016-0410-8>
- Wu TH, Gao YT, Zhou Y, Sun H (2021) A novel comprehensive quantitative method for various geological disaster evaluations in underground engineering: multidimensional finite interval cloud model (MFICM). *Environ Earth Sci* 80:696. <https://doi.org/10.1007/s12665-021-10012-1>
- Xu ZG, Xian MT, Li XF, Zhou W, Wang JM, Wang YP, Chai JR (2021) Risk assessment of water inrush in karst shallow tunnel with stable surface water supply: Case study. *Geomech Eng.* <https://doi.org/10.12989/gae.2021.25.6.495>
- Yang W, Jin L, Zhang X (2019) Simulation test on mixed water and sand inrush disaster induced by mining under the thin bedrock. *J Loss Prev Process Ind* 57:1–6. <https://doi.org/10.1016/j.jlp.2018.11.007>
- Yuan F, Shen T, Xie XS, Ma L, Wen XG (2021) Application of deep learning-based seismic multi-attribute fusion technology in the detection of water conducting fissure zone. *J Chin Coal Soc* 46(10):3234–3244
- Zhang GD, Xue YG, Bai CH, Su MX, Zhang K, Tao YF (2021a) Risk assessment of floor water inrush in coal mines based on MFIM-TOPSIS variable weight model. *J Cent South Univ* 28:2360–2374. <https://doi.org/10.1007/s11771-021-4775-x>
- Zhang J, Wu Q, Mu W, Du Y, Tu K (2019a) Integrating the hierarchy variable-weight model with collaboration-competition theory for assessing coal-floor water-inrush risk. *Environ Earth Sci* 78:1–13. <https://doi.org/10.1007/s12665-019-8217-0>
- Zhang QS, Wang DM, Li SC, Zhang X, Tan YH, Wang K (2017) Development and application of model test system for inrush of water and mud of tunnel in fault rupture zone. *Chin J Geotech Engin* 39(3):417–426
- Zhang WQ, Wang ZY, Shao JL, Zhu XX, Li W, Wu XT (2019b) Evaluation on the stability of vertical mine shafts below thick loose strata based on the comprehensive weight method and a fuzzy matter-element analysis model. *Geofluids* 2019:3543957. <https://doi.org/10.1155/2019/3543957>
- Zhang YW, Zhang LL, Li HJ, Chi BM (2021b) Evaluation of the water yield of coal roof aquifers based on the FDAHP-entropy method: a case study in the Donghuantuo coal mine. *China Geofluids* 2021:5512729. <https://doi.org/10.1155/2021/5512729>

**Publisher's Note** Springer Nature remains neutral with regard to jurisdictional claims in published maps and institutional affiliations.

Springer Nature or its licensor (e.g. a society or other partner) holds exclusive rights to this article under a publishing agreement with the author(s) or other rightsholder(s); author self-archiving of the accepted manuscript version of this article is solely governed by the terms of such publishing agreement and applicable law.